LOAN DOCUMENT

PHOTOGRAPH THIS SHEET

DTIC ACCESSION NUMBER

LEVEL

INVENTORY

WL-TR-96-2090

DOCUMENT IDENTIFICATION

DISTRIBUTION STATEMENT A
Approved for public release;
Distribution Unlimited

DISTRIBUTION STATEMENT

ACCESSION FOR
NTIS GRA&I
DTIC TRAC
UNANNOUNCED
JUSTIFICATION

BY
DISTRIBUTION/
AVAILABILITY CODES

DISTRIBUTION	AVAILABILITY AND/OR SPECIAL	
A-1		

DISTRIBUTION STAMP

DATE ACCESSIONED

DATE RETURNED

A-1 19960812 171

DATE RECEIVED IN DTIC

REGISTERED OR CERTIFIED NUMBER

PHOTOGRAPH THIS SHEET AND RETURN TO DTIC-FDAC

DTIC FORM 70A JUN 90

DOCUMENT PROCESSING SHEET

PREVIOUS EDITIONS MAY BE USED UNTIL STOCK IS EXHAUSTED.

LOAN DOCUMENT

HANDLE WITH CARE

DISCLAIMER NOTICE

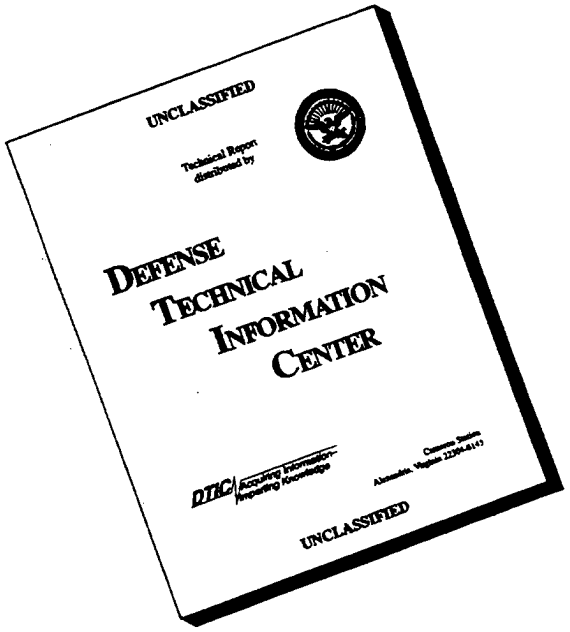

THIS DOCUMENT IS BEST QUALITY AVAILABLE. THE COPY FURNISHED TO DTIC CONTAINED A SIGNIFICANT NUMBER OF PAGES WHICH DO NOT REPRODUCE LEGIBLY.

WL-TR-96-2090

WALL-JET TURBULENT BOUNDARY LAYER HEAT FLUX, VELOCITY, AND TEMPERATURE SPECTRA AND TIME SCALES

David G. Holmberg
David J. Pestian

JUNE 1996

FINAL REPORT 1 NOVEMBER 1995--9 JULY 1996

Approved for public release; distribution unlimited

AERO PROPULSION & POWER DIRECTORATE
WRIGHT LABORATORY
AIR FORCE MATERIEL COMMAND
WRIGHT-PATTERSON AIR FORCE BASE, OH 45433-7650

NOTICE

WHEN GOVERNMENT DRAWINGS, SPECIFICATIONS, OR OTHER DATA ARE USED FOR ANY PURPOSE OTHER THAN IN CONNECTION WITH A DEFINITELY GOVERNMENT-RELATED PROCUREMENT, THE UNITED STATES GOVERNMENT INCURS NO RESPONSIBILITY OR ANY OBLIGATION WHATSOEVER. THE FACT THAT THE GOVERNMENT MAY HAVE FORMULATED OR IN ANY WAY SUPPLIED THE SAID DRAWINGS, SPECIFICATIONS, OR OTHER DATA, IS NOT TO BE REGARDED BY IMPLICATION, OR OTHERWISE IN any MANNER CONSTRUED, AS LICENSING THE HOLDER, OR ANY OTHER PERSON OR CORPORATION; OR AS CONVEYING ANY RIGHTS OR PERMISSION TO MANUFACTURE, USE, OR SELL ANY PATENTED INVENTION THAT MAY IN ANY WAY BE RELATED THERETO.

THIS REPORT IS RELEASABLE TO THE NATIONAL TECHNICAL INFORMATION SERVICE (NTIS). AT NTIS, IT WILL BE AVAILABLE TO THE GENERAL PUBLIC, INCLUDING FOREIGN NATIONS.

THE TECHNICAL REPORT HAS BEEN REVIEWED AND IS APPROVED FOR PUBLICATION.

RICHARD B. RIVIR
Manager, Aerothermal Research
Turbine Branch
Turbine Engine Division
Aero Propulsion & Power Directorate

CHARLES D. MACARTHUR
Chief
Turbine Branch
Turbine Engine Division
Aero Propulsion & Power Directorate

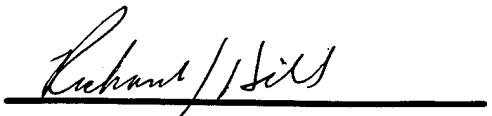

RICHARD J. HILL
Chief of Technology
Turbine Engine Division
Aero Propulsion & Power Directorate

IF YOUR ADDRESS HAS CHANGED, IF YOU WISH TO BE REMOVED FROM OUR MAILING LIST, OR IF THE ADDRESSEE IS NO LONGER EMPLOYED BY YOUR ORGANIZATION PLEASE NOTIFY WL/POTT, WPAFB OH 45433-7650 TO HELP MAINTAIN A CURRENT MAILING LIST.

REPORT DOCUMENTATION PAGE

Form Approved
OMB No. 0704-0188

1. AGENCY USE ONLY *(Leave blank)*	2. REPORT DATE	3. REPORT TYPE AND DATES COVERED
	JUNE 1996	Final 1 Nov 95 - 9 Jul 96

4. TITLE AND SUBTITLE

Wall-Jet Turbulent Boundary Layer Heat Flux, Velocity, and Temperature Spectra and Time Scales

5. FUNDING NUMBERS

PE 61102F
JON 2307S315

6. AUTHOR(S)

David G. Holmberg, David J. Pestian

7. PERFORMING ORGANIZATION NAME(S) AND ADDRESS(ES)

Aero Propulsion & Power Directorate
Wright Laboratory
Air Force Materiel Command
Wright-Patterson Air Force Base, OH 45433-7650

8. PERFORMING ORGANIZATION REPORT NUMBER

9. SPONSORING / MONITORING AGENCY NAME(S) AND ADDRESS(ES)

Aero Propulsion & Power Directorate
Wright Laboratory
Air Force Materiel Command
Wright-Patterson Air Force Base, OH 45433-7650
POC: Richard B Rivir, WL/POTT, 513-255-5132

10. SPONSORING / MONITORING AGENCY REPORT NUMBER

WL-TR-96-2090

11. SUPPLEMENTARY NOTES

12a. DISTRIBUTION / AVAILABILITY STATEMENT

APPROVED FOR PUBLIC RELEASE; DISTRIBUTION IS UNLIMITED

12b. DISTRIBUTION CODE

13. ABSTRACT *(Maximum 200 words)*

The interactions of boundary layer flow temperature fluctuations (t') and velocity fluctuations (u', v') together with surface heat flux fluctuations (q') have been investigated experimentally in a flat plate turbulent boundary layer in order to better understand time-resolved interactions between flow unsteadiness and surface heat flux. A Heat Flux Microsensor (HFM) was placed on a heated flat plate beneath a turbulent wall jet, and a split-film boundary layer probe was traversed above it together with a cold-wire temperature probe. The recorded simultaneous time-resolved u'v't'q' data can be correlated across the boundary layer. Results indicate that wall heat transfer (both mean and fluctuating components) is controlled by the u' fluctuating velocity field. In the presence of high free stream turbulence (FST), the heat flux is largely controlled by free stream eddies of large size and energy reaching deep into the boundary layer, such that heat flux spectra can be determined from the free-stream velocity field. This is evidenced by uq coherent present across the boundary layer, as well as by similarity in heat flux and a u velocity spectra, and by the presence of large velocity scales down to the nearest wall measuring location just above the laminar sublayer.

14. SUBJECT TERMS			15. NUMBER OF PAGES 9
			16. PRICE CODE
17. SECURITY CLASSIFICATION OF REPORT	18. SECURITY CLASSIFICATION OF THIS PAGE	19. SECURITY CLASSIFICATION OF ABSTRACT	20. LIMITATION OF ABSTRACT
UNCLASSIFIED	UNCLASSIFIED	UNCLASSIFIED	SAR

GENERAL INSTRUCTIONS FOR COMPLETING SF 298

The Report Documentation Page (RDP) is used in announcing and cataloging reports. It is important that this information be consistent with the rest of the report, particularly the cover and title page. Instructions for filling in each block of the form follow. It is important to ***stay within the lines*** to meet ***optical scanning requirements***.

Block 1. Agency Use Only *(Leave blank)*.

Block 2. Report Date. Full publication date including day, month, and year, if available (e.g. 1 Jan 88). Must cite at least the year.

Block 3. Type of Report and Dates Covered. State whether report is interim, final, etc. If applicable, enter inclusive report dates (e.g. 10 Jun 87 - 30 Jun 88).

Block 4. Title and Subtitle. A title is taken from the part of the report that provides the most meaningful and complete information. When a report is prepared in more than one volume, repeat the primary title, add volume number, and include subtitle for the specific volume. On classified documents enter the title classification in parentheses.

Block 5. Funding Numbers. To include contract and grant numbers; may include program element number(s), project number(s), task number(s), and work unit number(s). Use the following labels:

C	- Contract	**PR**	- Project
G	- Grant	**TA**	- Task
PE	- Program Element	**WU**	- Work Unit Accession No.

Block 6. Author(s). Name(s) of person(s) responsible for writing the report, performing the research, or credited with the content of the report. If editor or compiler, this should follow the name(s).

Block 7. Performing Organization Name(s) and Address(es). Self-explanatory.

Block 8. Performing Organization Report Number. Enter the unique alphanumeric report number(s) assigned by the organization performing the report.

Block 9. Sponsoring/Monitoring Agency Name(s) and Address(es). Self-explanatory.

Block 10. Sponsoring/Monitoring Agency Report Number. *(If known)*

Block 11. Supplementary Notes. Enter information not included elsewhere such as: Prepared in cooperation with...; Trans. of...; To be published in.... When a report is revised, include a statement whether the new report supersedes or supplements the older report.

Block 12a. Distribution/Availability Statement. Denotes public availability or limitations. Cite any availability to the public. Enter additional limitations or special markings in all capitals (e.g. NOFORN, REL, ITAR).

- **DOD** - See DoDD 5230.24, "Distribution Statements on Technical Documents."
- **DOE** - See authorities.
- **NASA** - See Handbook NHB 2200.2.
- **NTIS** - Leave blank.

Block 12b. Distribution Code.

- **DOD** - Leave blank.
- **DOE** - Enter DOE distribution categories from the Standard Distribution for Unclassified Scientific and Technical Reports.
- **NASA** - Leave blank.
- **NTIS** - Leave blank.

Block 13. Abstract. Include a brief *(Maximum 200 words)* factual summary of the most significant information contained in the report.

Block 14. Subject Terms. Keywords or phrases identifying major subjects in the report.

Block 15. Number of Pages. Enter the total number of pages.

Block 16. Price Code. Enter appropriate price code *(NTIS only)*.

Blocks 17. - 19. Security Classifications. Self-explanatory. Enter U.S. Security Classification in accordance with U.S. Security Regulations (i.e., UNCLASSIFIED). If form contains classified information, stamp classification on the top and bottom of the page.

Block 20. Limitation of Abstract. This block must be completed to assign a limitation to the abstract. Enter either UL (unlimited) or SAR (same as report). An entry in this block is necessary if the abstract is to be limited. If blank, the abstract is assumed to be unlimited.

WALL-JET TURBULENT BOUNDARY LAYER HEAT FLUX, VELOCITY, AND TEMPERATURE SPECTRA AND TIME SCALES

David G. Holmberg
Department of Mechanical Engineering
VA Tech, Blacksburg, VA

David J. Pestian
Aerospace Mechanics Division
UDRI, Dayton, OH

ABSTRACT

The interactions of boundary layer flow temperature fluctuations (t') and velocity fluctuations (u', v') together with surface heat flux fluctuations (q') have been investigated experimentally in a flat plate turbulent boundary layer in order to better understand time-resolved interactions between flow unsteadiness and surface heat flux. A Heat Flux Microsensor (HFM) was placed on a heated flat plate beneath a turbulent wall jet , and a split-film boundary layer probe was traversed above it together with a cold-wire temperature probe. The recorded simultaneous time-resolved u'v't'q' data can be correlated across the boundary layer. Results indicate that wall heat transfer (both mean and fluctuating components) is controlled by the u' fluctuating velocity field. In the presence of high free-stream turbulence (FST), the heat flux is largely controlled by free stream eddies of large size and energy reaching deep into the boundary layer, such that heat flux spectra can be determined from the free-stream velocity field. This is evidenced by uq coherence present across the boundary layer, as well as by similarity in heat flux and u velocity spectra, and by the presence of large velocity scales down to the nearest wall measuring location just above the laminar sublayer.

NOMENCLATURE

Nu/Nu_0	Ratio of experimental to theoretical Nusselt number, Nu=hx/k
Re_x	x Reynolds number, $U_{max}x/\nu$
Re_Δ	Enthalpy thickness Reynolds number.
Re_θ	Momentum thickness Reynolds number.
St/St_0	Ratio of experimental to theoretical Stanton number for low FST turbulent boundary layer, St=h/ρuc.
Tu_q	Heat flux turbulence intensity, q'/q
Tu_u	U velocity turbulence intensity, u'/u
Tu_t	Temperature turbulence intensity, t'/(t_{wall}-t_{max})
q, q'	Surface heat flux, and fluctuating component. (W/cm2)
t, t'	Temperature in boundary layer, and fluctuating component.
t^+	Near-wall dimensionless temperature $(t_{wall}-t)u_\tau \rho c / q$, where $u_\tau = (\tau_{wall}/\rho)^{1/2} = (c_f/2)^{1/2}$
t_m	Property reference temperature = $(t_{wall}+t_{max})/2$
u, u'	Streamwise velocity, and fluctuating component. (m/s)
u^+	Near-wall dimensionless velocity $(u/u_{max}) / (c_f/2)^{1/2}$
v, v'	Normal velocity, and fluctuating component. (m/s)
y^+	Near-wall dimensionless distance $(yu_{max}/\nu) / (c_f/2)^{1/2}$
δ_{995}	Boundary layer thickness.
Λ	Integral length scale. (mm)
τ	Integral time scale. (ms)
Δt	Temperature change across boundary layer, $t_{wall} - t_{max}$

subscript

max	Property taken at wall-jet maximum velocity point

INTRODUCTION

In the continuing effort to better understand heat transfer to turbine blading, much work has been done in recent years to elucidate heat transfer mechanisms and develop correlations to account for the effects of wake passing (due to upstream blade rows), transition (from laminar to turbulent boundary layer), free-stream turbulence (outside the boundary layer), acceleration (of the flow in the narrowing blade passages), length scales (some measure of turbulent eddy size), Reynolds number, etc. The work has generally fallen into three areas: transition, wake effects, and freestream turbulence (FST). Heat transfer is known to be highly sensitive to transition, and the variables that control transition are under continued study. The line between the effects of wakes and of FST is hazy, because FST after the first blade row exists only within a wake or between wakes. Except for the inlet flow to the first blade row, FST is primarily composed of lower frequency unsteadiness at the blade passing frequency, and higher frequencies due to the turbulent energy

estimated to be near 10%. Fluctuating heat flux, q', will not be affected as surface temperature is not changing.

Four channels with heat flux, u and v velocity, and cold-wire temperature were sampled by a National Instruments NB-A2150 board with data collected using LabVIEW software. The NB-A2150 samples simultaneously and filters data to remove aliasing. Data were post processed to convert from volts to calibrated units of heat flux, temperature and velocity. 8KB at 4kHz were sampled for each channel at 33 points across the boundary layer. Frequency data presented here are averaged 128 times.

Heat flux measurements were made using a Heat Flux Microsensor (HFM), Fig.2. The HFM consists of two sensors: a surface resistance temperature sensor (RTS) in a serpentine pattern (0.64cm in length), and a heat flux sensor (HFS, 1.85cm in length) stretching across the gage face. The HFM used in these tests (model HFM-2B-AlN-B from Thermoteq' Division of Vatell Inc.) was sputtered on an aluminum nitride ceramic disk with approximately the same thermal properties as the aluminum bar surrounding it, so that there is no thermal disruption due to the sensor's presence. The HFS consists of a thermopile with 100 pairs of Ni-Nichrome thermocouple junctions arranged above and below a thin (0.8μm) resistive layer so that heat flux is directly output (Holmberg, 1995). The RTS is a sputtered platinum wire driven by a 0.1mA current. Frequency response of both sensors is better than 100kHz (Holmberg, 1995). Calibration of the HFS was provided by the manufacturer (±10% uncertainty on the mean), while the RTS calibration was done in-situ.

Velocity measurements were made using a TSI model 1287 split-film seen in Fig.2. The sensor active length is 2.0mm, thus allowing resolution 10X that of the HFS, and the ability to see "mixing-length" scale (~0.1d) boundary layer turbulence. The cold-wire was a "home-made" wire (on a standard TSI Inc. U-wire probe body) with a wire etched down to a 0.5μm diameter, and driven in constant current mode to measure fluctuating temperature in the boundary layer. The active length is less than 0.2mm giving resolution 10X that of the split-film. The cold-wire was calibrated in-situ immediately after the completion of the test.

The cold-wire and split-film were displaced spanwise, Fig.2, to avoid interference of one in front of the other, but this led to reduced coherence due to this spatial separation, as will be seen. The probes were shown to significantly disturb wall heat flux values when near the wall. Heat flux measurements increased significantly at probe locations below 1mm due to flow distortion, with a 20% increase at the nearest location to the wall (0.2mm). Velocity measurements showed 2° of angular distortion at the wall, but it is not clear how much of this is due to potential flow distortion and how much to split film imbalance due to wall proximity to the lower film.

The HFS stretches across the face of the disk in a line to maximize axial resolution, and passes beneath both the split-film and cold-wire probes. As a result, coherence between velocity and heat flux (uq, vq) and between heat flux and cold-wire temperature (qt) is diminished at higher frequencies due to spanwise averaging across the HFS, and across the boundary layer probes as well. As mentioned above, coherence between velocity and temperature (ut, vt) is seriously affected by the probe separation, and this is especially evident near the wall where length scales are reduced.

TIME MEAN RESULTS

Mean velocity, and temperature profiles in dimensionless wall coordinates are shown in Figs. 3 and 4. The characteristic drop-off in the wake of a wall jet is seen in the u^+ vs. y^+ plot at large y^+. Temperature and velocity profiles are compared in Fig. 5 showing the less developed temperature profile. At the nearest probe, location (y^+=10), the velocity is 7 m/s and temperature 56°C (where t_{wall}= 101°C, t_{max}=28°C, and u_{max}=21.8 m/s) indicating the large temperature and velocity gradients across the laminar sublayer below y^+=10 (y=0.2mm). The enthalpy thickness (based on a variable property numerical integration) is only 1.0mm, where enthalpy thickness is an integral measure of the energy containing thickness of the boundary layer. Using air properties across the boundary layer based on the cold-wire temperature, and matching the log-layer to the Kays and Crawford (1980) correlation for a turbulent boundary layer ($u^+ = 5.6 \log_{10} y^+ + 4.9$), a skin friction value of c_f=0.0035 was found.

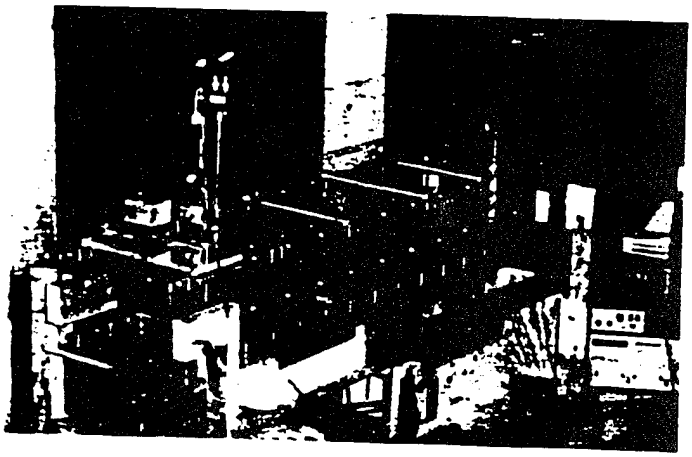

Fig.1 Wall-jet facility

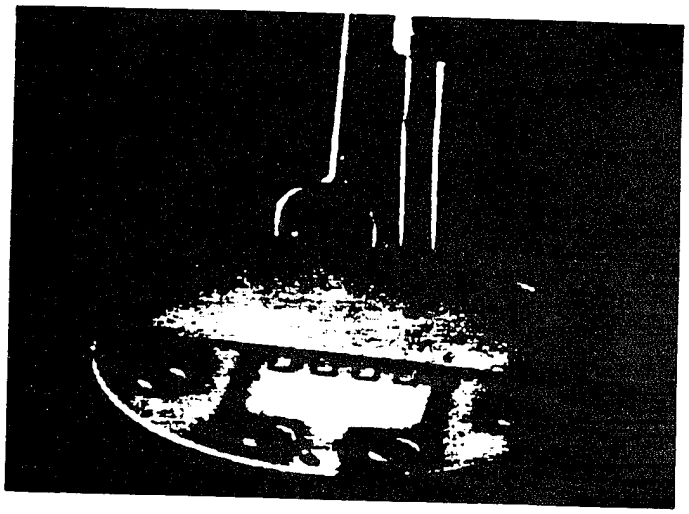

Fig.2 Probe arrangement above HFM

correlation for the heat transfer coefficient, h (W/m^2K) = 22.7 u' (m/s). Applying this to Rivir's data (to the accuracy allowed from his figures) as well as to the present data results in agreement between the two data sets, with the heat transfer coefficients based on respective u' both falling approximately 10% below Maciejewski's correlation.

TIME DOMAIN RESULTS

Some useful information can be gathered by looking at the time series across the boundary layer. Figure 7 shows simultaneous uvtq time traces near wall at y^+=10. Note the similarity in the u and q traces, with good coherence, and similar time scales, while q and t show limited coherence, which may be due to the much poorer resolution of the HFS. The v trace is near the noise floor (also seen in Fig.12), whereas t shows strong higher-frequency fluctuations. The development of u, v, and t are shown at three points across the boundary layer in Figs. 8, 9, and 10. Note that u does not change much in character above y^+=100, while v changes dramatically. Temperature fluctuations are strong near the wall, but die out away from the wall.

Table 1 gives integral time scales, length scales, and turbulence intensities across the boundary layer for u, v, t, and q. The classic turbulent boundary layer (low FST) has an eddy size equal to 0.41y out to 0.09δ. It is clear that this is not the case here by examining the Λ_u (integral length scale) column. Λu equals ymax (51mm) already at y^+=10, or just above the laminar sub-layer, but does peak near $0.4y_{max}$

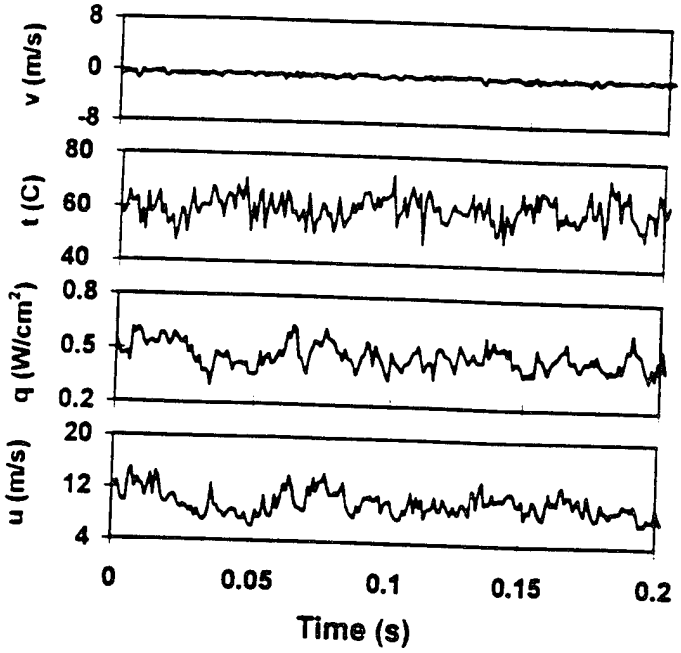

Fig.7 Comparisons of uvtq time series at y^+=10

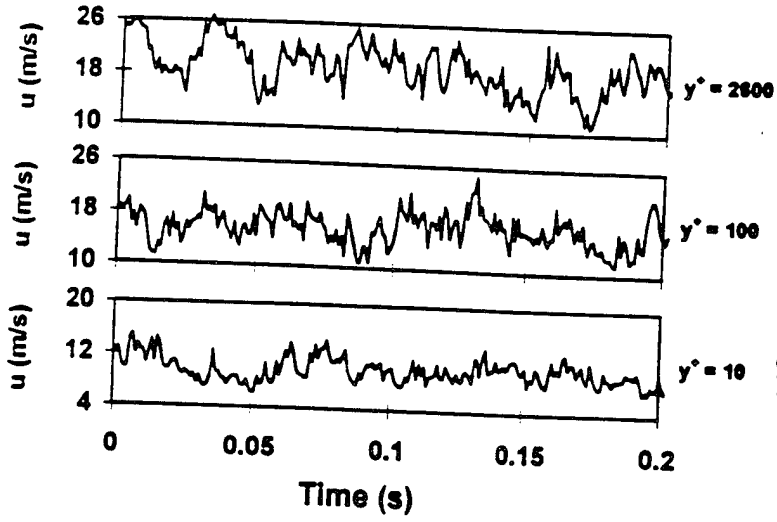

Fig.8 U velocity signal at y^+=10, 100, and 2600.

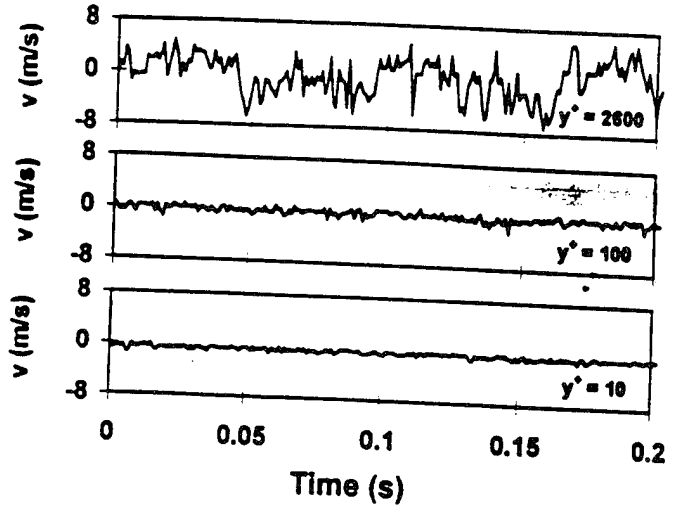

Fig.9 V velocity signal at y^+=10, 100, and 2600.

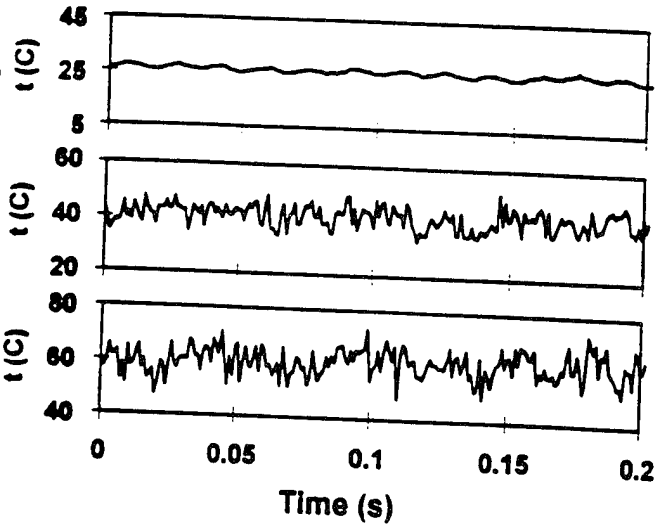

Fig.10 Temperature signal at y^+=10, 100, and 2600.

S_{tt}, Fig. 13, evidences the large decrease in temperature fluctuations across the log-region moving away from the heated wall. The high frequency fluctuations drop off more, indicating a decrease in smaller-scale temperature variations. This implies the diffusion of small high-energy eddies originating from near-wall activity (e.g. "bursting"), as well as the dominance of larger eddies (lower frequencies) that are responsible for moving the high enthalpy fluid away from the wall. 60Hz noise is buried in the strong near wall fluctuations, but evident away from the wall.

S_{qq}, Fig. 14, shows the change in the heat flux spectrum as the probe is traversed across the boundary layer. Without probe disturbance there would be no change in heat flux at the wall, but a small amount is evident. Note the drop off in the spectrum. The drop between 10 and 100 Hz of 10dB and between 100 and 1000Hz of 15 dB is equivalent to the drop in the u velocity spectrum despite the lower HFS resolution, again giving support to the scaling of q on u fluctuations. The 60Hz noise should be disregarded.

Second, examine the uq coherence and phase data in Figs. 15 and 16. The uq coherence across the boundary layer gives insight into the heat transfer mechanism. As expected, there is very good coherence near the wall and at lower frequencies, with coherence dropping off with distance from the wall and with frequency. Of note is that coherence is nearly zero at the maximum velocity point y^+=2600, but then increases slightly at y^+=4000. This may be an effect of large scale structures with spanwise vorticity rotating about the maximum velocity point. From the plot of uq phase, one can see that near the wall at y^+=10, and y^+=40 the u velocity and heat flux signals are in phase out to 200Hz (and could be expected to go out farther if not for probe spatial resolution issues), while at y^+=1200 the two signals are in phase only at the DC level, and then as frequency increases, heat flux lags velocity until they are 180 degrees out of phase at 150Hz. But at this point coherence is zero, and the phase fluctuations have become completely erratic. The phase lag grows even faster for points farther from the wall. Based on these plots we can see that q and u show high coherency across the entire log layer, with phase lag slowly increasing with distance from the wall. Only in the wake region is coherence lost.

The vq coherence, Fig. 17, shows a complementary profile. The coherence in the lower part of the log layer is zero, while out at y^+=1200 and beyond the coherence is significant. The vq phase, Fig. 18, reveals that at y^+=1200 there is some phase agreement. This appears to support a "splat" phenomena where v energy is

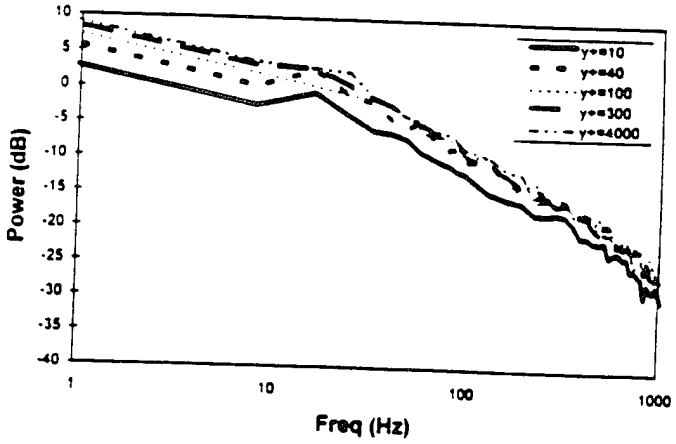

Fig.11 U autospectrum across boundary layer

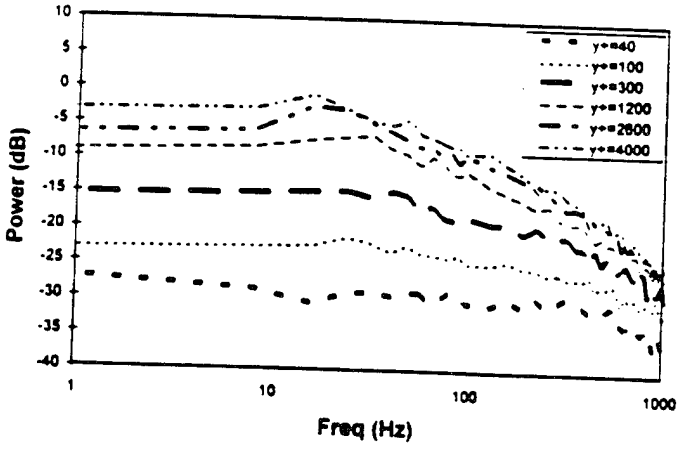

Fig.12 V autospectrum across boundary layer

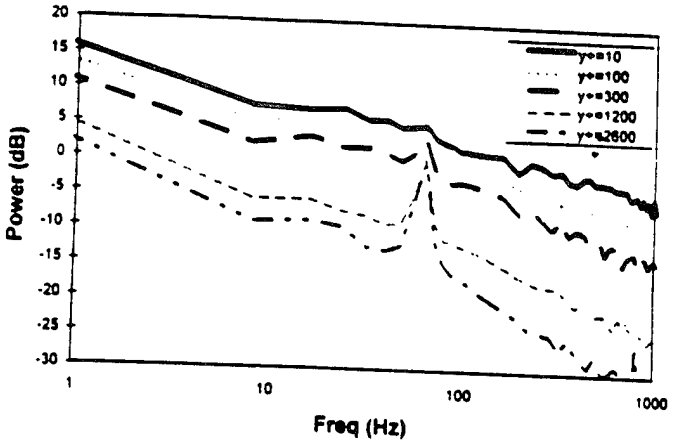

Fig.13 Temperature autospectrum across boundary layer

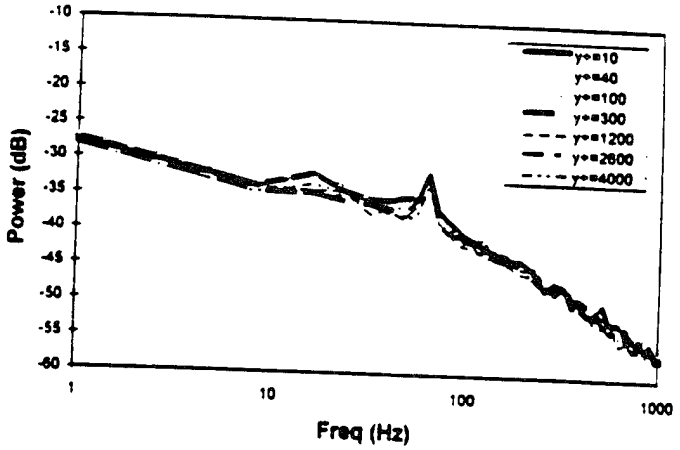

Fig.14 Heat flux autospectrum across boundary layer

to convected temperature variations primarily in the u direction. It seems likely that the coherence between q and t is a combination of large eddies from outside the boundary layer (seen here) and higher frequency bursts from the wall region (not seen here).

Based on the above discussion it is clear that whatever near-wall small-scale activity may be present and responsible for heat transfer across the lower 4% of the boundary layer ($y^+<100$), outside of this inner region heat transfer is dominated by large freestream turbulence reaching deep into the boundary layer and controlling the observed heat flux. It is also evident that the large increases in heat transfer over low-FST due to the presence of high-FST are due to these large freestream eddies reaching into the boundary layer, adding energy and enhancing the mixing of wall fluid into the freestream. This also explains the observed scaling of heat transfer on velocity fluctuations.

CONCLUSION

The interactions of cold-wire temperature (t') and split-film velocity fluctuations (u', v') together with surface heat flux fluctuations (q') from a Heat Flux Microsensor have been investigated experimentally in a wall-jet facility. Mean results give $St/St_0 \cong 1.2$ which is near the enhancement due to the presence of FST that is predicted by existing correlations which base length scale effects on the enthalpy thickness. However, similar data from another 2-D wall-jet facility gives $St/St_0 \cong 2.0$. This disagreement is resolved by dismissing St correlations, based on mean velocity, and instead basing the heat transfer coefficient strictly on the fluctuating velocity component, u'.

This scaling of heat flux on velocity fluctuations is seen not only in the mean heat transfer, but also in time-resolved measurements. In the presence of high FST, the heat flux is largely controlled by free stream eddies of large size and energy reaching deep into the boundary layer. This is evidenced by the uq coherence present across the boundary layer, as well as by the similarity in heat flux and u velocity spectra, and by the integral time scale τ_u which remains nearly constant across the boundary layer even at the nearest wall measuring location just above the laminar sublayer. Whatever small-scale wall activity (e.g. "bursting") that may be present is not relevant in relating heat transfer to free-stream phenomena. Or in other words, knowledge of the fluctuating velocity field outside the boundary layer can be used to determine the frequency spectra of the heat flux, as well as mean heat flux levels.

In summary, wall heat transfer is controlled by the u velocity field. Large freestream eddies reaching down into the boundary layer cause near wall fluctuations in u, as well as mixing in the boundary layer. The heat flux spectrum matches the velocity spectrum in its distribution of energy, with similar time scales, and high coherence at the wall.

ACKNOWLEDGMENTS

The use of Dr. Richard Rivir's Turbine Aerothermal Research Laboratory of the Turbine Branch (WL/POTT) at Wright Lab at Wright Patterson AFB, and his support in modifying the wall-jet facility and subsequent guidance is greatly appreciated. The assistance of Mr. Greg Cala is also appreciated. The work was made possible as part of the Air Force Laboratory Graduate Fellowship, with funding administered through the office of Prof. Peele of the Southeastern Center for Electrical Engineering Education.

REFERENCES

Ames, F.E., and Moffat, R.J., 1990, "Heat Transfer with High Intensity, Large Scale Turbulence: The Flat Plate Turbulent Boundary Layer and the Cylindrical Stagnation Point," Report No. HMT-44, Thermosciences Division of Mechanical Engineering, Stanford University.

Ames, F.E., 1994, "Experimental Study of Vane Heat Transfer and Aerodynamics at Elevated Levels of Turbulence," NASA CR-4633.

Arts, T., Lambert de Rouvroit, M., 1992, "Aero-Thermal Performance of a Two-Dimensional Highly Loaded Transonic Turbine Nozzle Guide Vane: A Test Case for Inviscid and Viscous Flow Computations," JT, Vol.114, p.147.

Ashworth, D.A., LaGraff, J.E., Schultz, D.L., 1989, "Unsteady Interaction Effects on a Transitional Turbine Blade Boundary Layer," JT, Vol.111, p.162.

Dullenkopf, K., Mayle, R.E., 1994, " An Account of Free-Stream Turbulence Length Scale on Laminar Heat Transfer," ASME Paper 94-GT-174.

Dunn, M.G., Seymour, P.J., Woodward, S.H., George, W.K., Chupp, R.E., 1989, "Phase-Resolved Heat-Flux Measurements on the Blade of a Full-Scale Rotating Turbine," JT, Vol.111, p.8.

Garside, T., Moss, R.W., Ainsworth, R.W., Dancer, S.N., Rose, M.G., 1994, "Heat Transfer to Rotating Turbine Blades in a Flow Undisturbed by Wakes," IGTI Aeroengine Congress and Expo, The Hague, Netherlands, ASME 94-GT-94.

Guenette, G.R., Epstein, A.H., Giles, M.B., Haimes, R., Norton, R.J.G., 1989, "Fully Scaled Transonic Turbine Rotor Heat Transfer Measurements," JT, Vol.111, p.1.

Holmberg, D.G., Diller, T.E., 1995, "High-Frequency Heat Flux Calibration and Modeling," J. Fluids Engineering, Vol.117.

Kays, W.M., and Crawford, M.E., 1980, Convective Heat and Mass Transfer, 2nd Ed., McGraw-Hill, Inc., N.Y.

Keller, F.J., Wang, T., 1994, "Flow and Heat Transfer Behavior in Transitional Boundary Layers with Streamwise Acceleration," ASME Paper 94-GT-24.

Kim, J., Simon, T.W., Russ, S.G., 1992, "Free-Stream Turbulence and Concave Curvature Efffects on Heated Transitional Boundary Layers," JHT, Vol.114, p.339.

Maciejewski, P.K., 1995, "Limitations to the Employment of Conventional Boundary Layer Parameters and Predictive Models to Heat Transfer in Complex Flows," in Heat Transfer in Turbulent Flows, Eds. N.K. Anand et.al., ASME, NY, pp.37-44.

Mayle, R.E., 1991, "The Role of Laminar - Turbulent Transition in Gas Turbine Engines," JT, Vol.113, p.509.

Moss, R.W., and Oldfield, M.L.G., 1992, "Measurements of the Effect of Free-Stream Turbulence Length Scale on Heat Transfer," ASME Paper 92-GT-244.

Moss, R.W., and Oldfield, M.L.G., 1994, "Effect of Free-Stream Turbulence on Flat-Plate Heat Flux Signals: Spectra & Eddy Transport Velocities," ASME Paper 94-GT-205.